

STUDY OF MAGNETIC HARDENING IN $\text{Sm}(\text{Co}_{1-x}\text{Cu}_x)_5$ ALLOY

*M. S. AWAN, A. S. BHATTI and M. FAROOQUE

Department of Physics, COMSATS Institute of Information Technology, Park Road, Islamabad, Pakistan

(Received July 28, 2008 and accepted in revised form December 17, 2008)

Magnetic hardening has been examined in the samarium (Sm), cobalt (Co) and copper (Cu) fused permanent magnets by correlating the magnetic properties with annealing temperature and microstructure of the samples. For the $\text{Sm}(\text{Co}_{1-x}\text{Cu}_x)_5$ system, with various copper contents ($x=0, 0.2, 0.3, 0.4$ and 0.5) the shape of initial magnetization curve indicated that the magnetic hardening process involved in these types of magnets consists of domain wall pinning type. This is consistent with the microstructure studies which show the existence of nonmagnetic Cu-rich precipitates in the Co-rich matrix. Copper substituted samples were annealed in the temperature range ($300 - 1000$) °C for 3h under the protective atmosphere of argon (Ar) gas. Both cast and annealed samples prepared by tri-arc melting technique exhibit two-phase microstructure responsible for enhanced magnetic properties. Metallographic and surface studies were carried out using a digital optical microscope (OM). X-ray diffraction (XRD) studies confirmed that the alloys solidified in the hexagonal crystal structure. The lattice parameters and unit cell volume increase with increasing Cu content. Scanning electron microscope (SEM) coupled with energy dispersive X-ray (EDX) was used to examine the surface morphology, compositional variations, elemental segregations, formation and effect of annealing on the different phases. Later these parameters were related to the magnetic properties. Copper-rich phase precipitates in the Co-rich matrix may serve as the pinning centers for the domain wall motion. Introduction of these pinning centers improved the magnetic hardening of the alloy. Annealing the Cu-substituted alloy further improved the magnetic properties. During annealing, diffusion of copper played the key role for enhanced magnetic properties. It was found that both Cu substitution and subsequent annealing are the dominating factors determining the magnetic properties of these magnetic alloys.

Keywords: Permanent magnets, $\text{Sm}(\text{Co}_{1-x}\text{Cu}_x)_5$, Coercivity, Magnetic hardening, Residual induction, Domain wall pinning, Magnetic alloy

1. Introduction

Modern permanent magnet devices require large coercive forces and high Curie temperatures to operate at higher temperatures. This demands the presence of magnetocrystalline anisotropy. Favorable candidates are rare-earth and 3d-transition metals due to their large magnetocrystalline anisotropy and high Curie temperatures, respectively. Large magnetocrystalline anisotropy in rare-earths originates from interaction of the crystal field and asymmetry of the charge cloud of the 4f electrons. 3d transition metals (Mn, Fe, Co and Ni) have large magnetization and Curie temperatures. Interaction of the magnetic moments of 3d electrons with the magnetic moments, associated with the rare-earth elements constitutes the basis of magnetic ordering and of the magnetic crystal anisotropy, essential for these modern permanent magnets. Their combination yields well defined intermetallic compounds with superior magnetic properties. Of these, RCO_5 and R_2Co_{17} (R

is lighter rare-earth element) compounds are of great interest. The RCO_5 (R=Sm) compound has moderate value of saturation magnetization (1T) but extremely large value of magnetocrystalline anisotropy constant (17 MJ/m^3) whereas 2:17 compound exhibits higher saturation magnetization (1.5T) but considerably smaller value of magnetocrystalline anisotropy constant (3 MJ/m^3) [1].

RCO_5 compounds have hexagonal crystal structure [2-3] and are strong candidates for the fine-particle magnets due to their strong magnetocrystalline anisotropy [4-5]. Taking the advantage of low saturation magnetization, SmCo_5 compound can be further explored for better magnetic properties. The physical and magnetic properties of as-cast 1:5 compound are poor enough to be used as permanent magnet. So it is necessary to modify the compound by grinding into fine particles [6-8]. During fine-particle powder preparation, some difficulties arise: like oxidation

* Corresponding author : sss_awan@yahoo.com

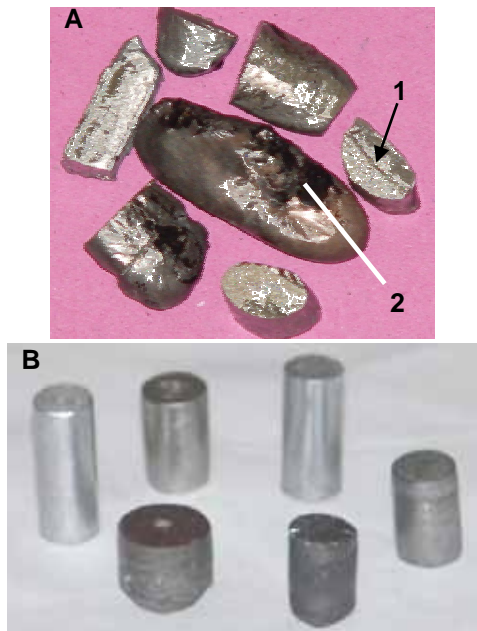


Figure-1 As-cast samples of SmCoCu (A) irregular ingots showing 1-fracture surface 2-Sm-rich thin blackish layer (B) cast regular cylindrical ingots.

of the fine powder due to large surface and loss of coercive force during grinding [9-11] and of course the technology behind the powder metallurgy is too expensive. To avoid these difficulties various methods have been adopted to produce permanent magnets without grinding by a number of researchers [12-18].

The main objective of this study was to improve the magnetic properties of as-cast SmCo₅ alloy. For this purpose alloy addition technique was adopted and Co was partially replaced with Cu according to the formula Sm(Co_{1-x}Cu_x)₅ where x= 0, 0.2, 0.3, 0.4 and 0.5. The role of annealing is also investigated by heat treating the samples after casting under inert atmosphere.

2. Experimental

A number of alloy ingots of binary and ternary compositions Sm(Co_{1-x}Cu_x)₅ were prepared with x=0, 0.2, 0.3, 0.4 and 0.5. Arc melting technique was applied to prepare the alloy buttons of irregular shape as shown in Figure 1. The purity of the metals (Sm, Co and Cu) was 99.99%. Melting pot was a hemispherical copper hearth. Melting was carried out under the dynamic flow of the argon gas in order to avoid the oxidation of the alloy. During melting and casting due to high vapour pressure samarium evaporates and come



Figure-2. Alloy ingot encapsulated in the quartz tube back filled with argon gas.(A) before heat treatment (B) after heat treatment

on to the surface as a thin blackish layer as shown in Figure 1(a). This may alter the original composition of the alloy. Additional samarium was optimized [19] to be ~6%. For magnetic measurements the limitation of the magnetometer was to have regular shape of the sample. So, copper hearth was modified to get the regular cylindrical shape of samples as shown in Figure 1(b). Samples were annealed in the temperature range (300-1000) °C/3h and then furnace cooled. Before any heat treatment the samples were sealed in quartz tube under Ar atmosphere as shown in Figure 2. A small piece of samarium was added in the tube to reduce the evaporation losses. Each time during sealing, first quartz tube was evacuated to 10⁻⁵ mbar and then back filled with Ar at atmospheric pressure. In order to make sure that maximum oxygen has been replaced by Ar, the quartz tube was flushed 2-3 times. Finally, the sample alongwith samarium piece was sealed under Ar at proximately atmospheric pressure.

For surface morphology and metallographic studies, samples were mold mounted, ground, polished and finally etched in a solution containing (3:1:1) glycerin, acetic acid and nitric acid (HNO₃) respectively. Surface studies and chemical analysis were performed on digital Olympus optical and Jeol JSM-5910LV scanning electron microscope (SEM)-equipped with Oxford EDX-system. For structural analysis XRD measurements were taken on bulk samples using Siemens D-500 X-ray diffractometer equipped with four-circle goniometry. Co-K α radiations ($\lambda=1.79021$ Å) were used for scanning. Magnetic measurements were performed on a Riken Denshi DC-BHU-30 B-H curve tracer. During measurements the maximum attainable magnetic field strength was limited to 20kOe.

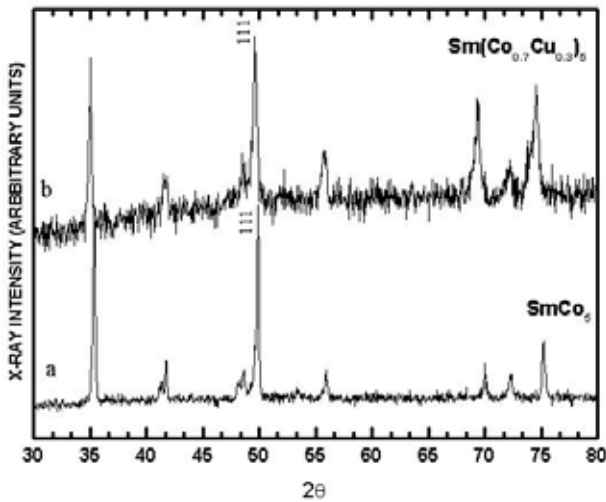


Figure 3. XRD patterns of the as-cast alloys of (A) SmCo_5 and (B) $\text{Sm}(\text{Co}_{0.7}\text{Cu}_{0.3})_5$.

3. Results and Discussion

Figure 3(a-b) is the X-ray diffraction patterns of the as-cast alloys of SmCo_5 and $\text{Sm}(\text{Co}_{0.7}\text{Cu}_{0.3})_5$ compositions. All the peaks were compared with the standard JCPD cards (PDF No. 35-1400 for

SmCo_5 and PDF No. 23-0934 for $\text{Sm}(\text{Co}_{0.7}\text{Cu}_{0.3})_5$) and indexed. The highest intensity peak for both the as-cast alloys was obtained for the reflection from (111) plane. The as-cast alloys during solidification follow the hexagonal crystal structure with space group $P6/mmm$ [19]. Comparing the XRD patterns it is observed that there is a slight shift in the (111) reflection peak. This peak is shifted towards the lower 2θ -value for the copper containing alloy. This may be due to the incorporation of the copper atoms into the lattice of 1:5 unit cells [20]. This was also confirmed when lattice parameters were determined for both the compositions. There was a slight increase in the c-axis of the copper containing alloy when compared with the SmCo_5 alloy [21-23]. Hence there is an increase in the volume of unit cell with increasing Cu content. This may be due to the fact that radius of the Cu atom is larger than that of the Co atom [24].

The as-cast samples of $\text{Sm}(\text{Co}_{1-x}\text{Cu}_x)_5$ show a strong tendency to micro segregation [25] and even after long time annealing, no homogenization

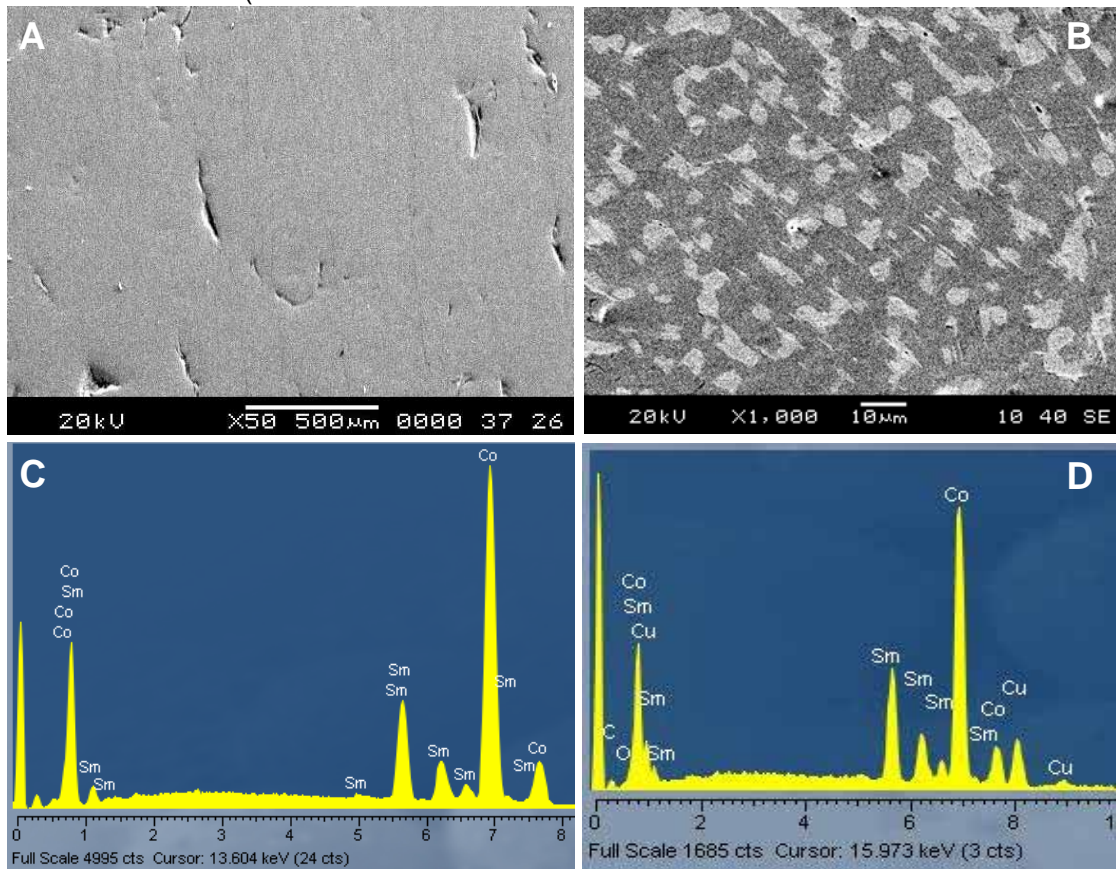


Figure 4. SEM micrographs of the as-cast alloys (A) SmCo_5 showing single phase microstructure with cracks (B) $\text{Sm}(\text{Co}_{0.7}\text{Cu}_{0.3})_5$ showing two-phase microstructure (C) EDX-Spectrum of the SmCo_5 alloy (D) EDX-spectrum of $\text{Sm}(\text{Co}_{0.7}\text{Cu}_{0.3})_5$ alloy.

could be achieved which is in agreement with previous reports [19-26]. Figure 4(A-D) shows SEM micrographs and EDX spectrums of the as-cast alloys with and without copper addition. It is observed that addition of copper ($x=0.3$) brought about an interesting apparent network change in the texture of SmCo_5 alloy. The cracks are almost vanished. The binary alloy SmCo_5 exhibits single-phase whereas the ternary $\text{Sm}(\text{Co}_{0.7}\text{Cu}_{0.3})_5$ alloy exhibits two-phase microstructure as shown in Figure 4 (A and B). EDX analysis confirms the single and two phase nature of the binary and ternary alloys. Figure 2(C and D) are the EDX spectrums from the respective alloys. For copper substituted sample (Figure 2B) white paths and plane gray areas are the copper and cobalt rich areas. The detailed elemental analysis by EDX from these areas is given in Table 1.

Table-1 EDX analysis (Wt.%) of as-cast and annealed (700°C/3h) samples of $\text{Sm}(\text{Co}_{1-x}\text{Cu}_x)_5$ with $x=0$ and 0.3.

Sample		Area	Co	Cu	Sm
As - cast	SmCo_5		66.21		33.78
	$\text{SmCo}_{0.7}\text{Cu}_{0.3}$	Cu-rich	35.74	27.82	36.45
		Co-rich	48.04	18.54	33.40
Annealed	$\text{SmCo}_{0.7}\text{Cu}_{0.3}$	Cu-rich	22.41	38.31	39.46
		Co-rich	48.88	17.57	33.52

Copper substitution has a remarkable effect on the structural and magnetic properties of cast SmCo_5 alloy. Figure 5 shows the first and second quadrants of the MH-loops of $(\text{SmCo}_{1-x}\text{Cu}_x)_5$ alloy with various copper contents ($x= 0, 0.2, 0.3, 0.4$ and 0.5) for as-cast alloys. The trend of MH-loops (for various copper contents) shows that with copper addition there is an improvement in the magnetic properties at the cast of maximum magnetization (M_{max}). For the sample with $x=0$, the shape of initial magnetization curve (red) is such that material is spontaneously magnetized as

magnitude of the external field is increased and finally saturation is achieved. Introduction of copper changed the shape of initial magnetization curve. Copper containing alloys do not magnetize spontaneously. Starting portions of the initial magnetization curves show that there is no influence of the external magnetic field upon the magnetization of the alloys. As magnitude of the external magnetic field increases eventually magnetization starts and finally samples are saturated. Resistance for magnetization in the initial magnetization curve continuously increases by increasing the copper contents. This is due to the fact that introduction of copper perhaps pinned the magnetic moments and domain wall motion. As a result it is not easier for the moments to align in the direction of the external magnetic field. The shape of initial magnetization curves clearly indicates a uniform domain wall pinning process [27] in these types of magnets.

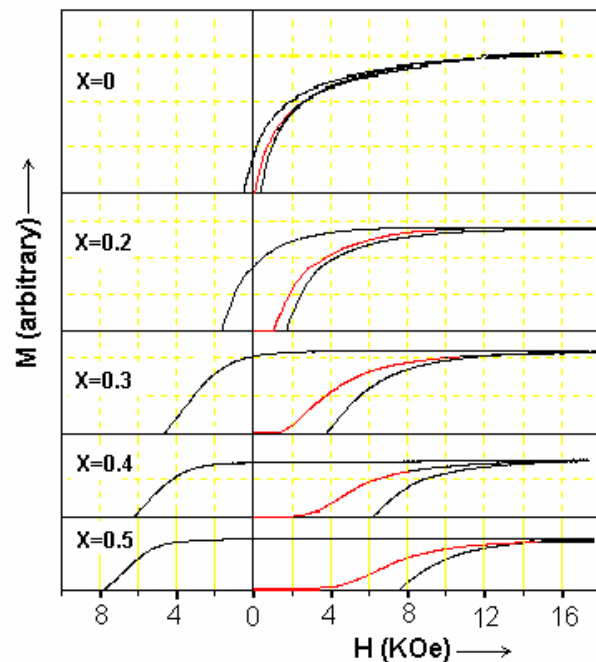


Figure 5. First and second quadrants of MH-loops showing magnetic properties as a function of copper contents for the $\text{Sm}(\text{Co}_{1-x}\text{Cu}_x)_5$ with ($x=0, 0.2, 0.3, 0.4$ and 0.5). Loops also include the virgin (initial magnetization) curves.

Annealing of cast samples introduces the interesting precipitation network as shown in Figure 6. Samples $\text{Sm}(\text{Co}_{1-x}\text{Cu}_x)_5$ with $x=0.3$ were annealed in the temperature range (300-1000)°C for three hours and then furnace cooled. Annealing was carried out under argon atmosphere in order to avoid the oxidation of the alloy. There is

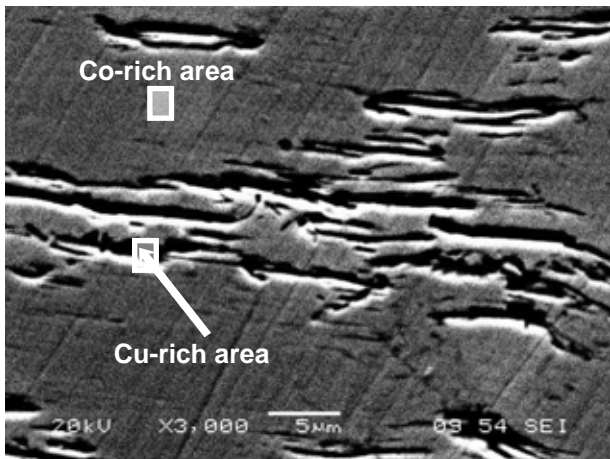


Figure 6 SEM micrograph of the sample $\text{Sm}(\text{Co}_{1-x}\text{Cu}_x)_5$ with $x=0.3$ annealed at $700^\circ\text{C}/3\text{h}$ under argon atmosphere.

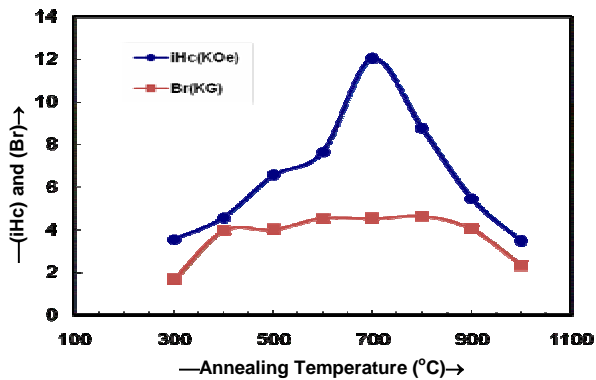


Figure 7 Magnetic properties (H_c and B_r) as a function of annealing temperature.

remarkable increase in the magnetic properties due to annealing. Figure 7 shows the magnetic properties (H_c and B_r) as a function of annealing temperature. These graphs show that annealing largely affected the H_c as compared to B_r . A maxima of H_c is reached for annealing at $700^\circ\text{C}/3\text{h}$. After annealing the sample showed two-phase microstructure with different microchemistry. Etched texture shows that elongated black copper rich precipitates are randomly distributed in the cobalt rich matrix as shown in Figure 6 for the sample with $x=0.3$ annealed at $700^\circ\text{C}/3\text{h}$. The chemical composition by EDX analysis of this sample is given in Table 1. EDX analysis shows that most of the copper during annealing diffused from Co-rich phase to Cu-rich phase. This makes the Cu-rich phase more and more nonmagnetic. So it better to isolate the magnetic Co-rich areas. This may give the better pinning effect to the domain wall motions. Hence the presence of copper rich precipitates may

effectively pin the domain wall motion [13]. Y. Zhang [28] proposed that Cu addition in SmCo_5 may disorder the crystal structure in localized region of 1:5 matrix. These disordered regions may serve as domain wall pinning sites. As a result H_c for this sample increase from 4249 Oe to 12032 Oe after annealing at 700°C for three hours.

4. Conclusions

The partial replacement of Co with Cu in the $\text{Sm}(\text{Co}_{1-x}\text{Cu}_x)_5$ system results in a two-phase microstructure which yields magnetically stronger alloy. The virgin magnetization curves indicate that the domain wall pinning is the operative magnetic hardening process in these types of magnets. Annealing as-cast samples modifies the microstructure and microchemistry of the alloys. During annealing diffusion of Cu from Co-rich phase to Cu-rich phase creates a large domain-wall energy gradient which magnetically isolate the two phases and improves the magnetic properties. Lower Cu contents $0.3 \geq x > 0$ favours the magnetic properties of both as-cast and annealed samples.

References

- [1] G.Y. Chin, Science **208** (1980) 23.
- [2] J.H. Wernick and S. Geller, Acta Cryst. **12** (1959) 662.
- [3] S.E. Haszoka, Trans. Met. Soc. AIME **218** (1960) 763.
- [4] G. Hoffer and K. Strnat, J. Appl. Phys. **38** (1967) 1377.
- [5] K. Strnat, G. Hoffer, J. Olson, W. Ostertag and J.J. Beaker, J. Appl. Phys. **38** (1967) 1001.
- [6] D.K. Das: IEEE Trans. On Magnetics **Mag-5**, No. 3, (1969) 214.
- [7] K.H.J. Buschow, W. Luiten, P.A. Naastepad and F.F. Westendorp, Philips Technical Review **29**, No. 11 (1968) 336.
- [8] K.H.J. Buschow, P.A. Naastepad and F.F. Westendorp J. Appl. Phys. **40**, No. 10, (1969) 4029.
- [9] K.J. Strnat, J.C. Olson and G. Hoffer, J. Appl. Phys. **39** (1968) 1263.
- [10] K.J. Strnat, J.C. Olson and G. Hoffer, Proc. 6th Rare-earth Res. Conf. (Gotlinburg, Tenn) (1967) p. 603-614.

- [11] K.J. Strnat, G. I. Hoffer, J.C. Olson and R.W. Kubach, IEEE Trans. Magnetics, Mag-4 (1968) 255.
- [12] T.J. Cullen, J. Appl. Phys. **42**, No. 4 (1971) 1535.
- [13] F. Hofer: IEEE Trans. On Magnetic **Mag-6**, No. 2 (1970) 221.
- [14] E.A. Nesbitt, R.H. Willens, R.C. Sherwood, E. Buehler and J.H. Wernick, Appl. Phys. Lett. **12**, No. 11 (1968) 361.
- [15] A.M. Yelon and E.A. Nesbitt, J. Appl. Physics **40**, No. 3 (1969) 1259.
- [16] E.A. Nesbitt, R.H. Willens, R.C. Sherwood, E. Buehler and T.W. Wernick, Appl. Phys. Lett., **12** (1968) 361.
- [17] Y. Tawara and H. Senno, J. Appl. Phys. **7** (1968) 966.
- [18] E.A. Nesbitt, J. Appl. Phys. **40** (1969) 1259.
- [19] P. Kersch, A. Handstein, K. Khlopov, O. Gutfleisch, D. Eckert, K. Nenkov, J.C. Tellez-Blanco, R. Grossinger, K.H. Muller and L. Schultz, J. Magn. Mag. Mater. **290-291** (2005) 420.
- [20] J.C. Tellez-Blanco, R. Grossinger, R. Sato Turtelli: Journal of Alloys and Compounds **281** (1998) 1.
- [21] F. Meyer-Liautaud, S. Derkaoui, C.H. Allibert, R. Castanet, J. Less-Common Met. **127** (1987) 231.
- [22] K.H.J. Buschow, A.S. Van der Goot, J. Less-Common Met. **14** (1968) 323.
- [23] I. Nishida, M. Uehara, J. Less-Common Met. **34** (1974) 285.
- [24] J. Luo¹, J.K. Liang, Y.Q. Guo, Q.L. Liu, L.T. Yang, F.S. Liu, G.H. Rao and W. Li: J. Phys.: Condens. Matter **15** (2003) 5621.
- [25] K.J. Strant: IEEE Trans. On Magnetics, **MAG-6**, No. 2 (1970) 191.
- [26] E. Estevez-Rams, J. Fidler, A. Valor-Reed, J.C. Tellez-Blanco, R. Sato Turtelli, R. Grossinger: J. Magn. Magn. Mat. **195** (1990) 595.
- [27] G.C. Hadjipanayis: Soft and Hard Magn. Mat. Symp. Proc. Orlando (1986).
- [28] Y. Zhang, A. Gabay, Y. Wang, and G.C. Hadjipanayis, J. Magnetism and Magnetic Materials **272** (2004) e1899.